Achieving Doppler Resilience of Mismatched Complementary-on-Receive Filtering (MiCRFt)

Alex C. Woods, David G. Felton, Jonathan W. Owen, Matthew B. Heintzelman, Shannon D. Blunt
Radar Systems Lab (RSL), University of Kansas, Lawrence, KS

***Abstract*—The utility of complementary-coded waveforms has historically been limited due to the fundamental disconnect between theory and practical implementation. Transmitter distortions (e.g. amplifier memory effects) particularly distort phase-codes, while Doppler sensitivity poses feasible limitations outside purely static environments. To address the former, the notion of mismatched complementary-on-receive filtering (MiCRFt) was recently introduced to suppress range sidelobes via subset combining of pulse-compressed responses, albeit only mitigating range-sidelobe modulation (RSM) caused by zero-Doppler scattering.**

Here, the MiCRFt framework is extended to achieve complementary sidelobe suppression across a prescribed Doppler span. This Doppler-generalized MiCRFt (DG-MiCRFt) framework demonstrates complementary enhancement via receive filter design for arbitrary sets of dissimilar waveforms (having similar spectral support). Importantly, the complementary operation is not limited by transmit design requirements and thus simplifies physical realization, for < 3 dB of mismatch loss. The efficacy of DG-MiCRFt filtering is assessed with simulation results and loopback hardware measurements.

Keywords—complementary waveforms, mismatched filtering, waveform diversity

I. INTRODUCTION

The notion of complementary radar waveforms has been explored since the original proposal by Golay [1]. Specifically, the idea involves designing signals with autocorrelations that during receive processing sum to produce (theoretically) zero sidelobes. However, their operational use has been hindered by two practical aspects: unavoidable transmitter distortion (especially at high-power) and degraded sidelobe cancellation outside of the zero Doppler response [2].

Traditional complementary sequences were posed as phase-coded signals, which can possess large, abrupt phase transitions and therefore entail poor spectral containment, ultimately translating to a discrepancy between theoretical design and physical realization in radar hardware. Some work has been done [3][4] to address the Doppler dependence of complementary cancellation, though the reliance on phase-codes still limits their physical implementation in hardware.

Alternatively, the complementary frequency modulated (Comp-FM) approach developed in [3] addressed the transmitter distortion limitation by iteratively optimizing uniquely-modulated, spectrally-contained random-FM waveforms in subsets to suppress sidelobes via complementary presumming prior to slow-time processing. While this approach was limited to complementary cancellation at zero-Doppler, [5] subsequently extended [3] to realize a Doppler-Generalized (DG) form of Comp-FM that provides a depth versus width cancellation trade-off over a wider Doppler span.

A completely different approach to complementary sidelobe cancellation was taken in [6] in which the mismatched complementary-on-receive filtering (MiCRFt) formulation was shown to achieve this effect for arbitrary nonrepeating waveforms. Mismatched filters (MMF) represent a deviation from standard matched filtering, with suppression of range sidelobes accomplished in exchange for mismatch loss (MML). The MiCRFt formulation jointly optimizes MMFs for a subset of Z distinct waveforms (having similar spectral support), with the presummed composite pulse compression response of the Z signal/filter pairs significantly reducing sidelobes relative to a single signal/filter basis (i.e., when $Z = 1$, which simplifies to a standard least-squares MMF). However, the original MiCRFt formulation only addressed zero-Doppler, with the presence of meaningful Doppler inducing a reversion to the no-cancellation condition of incoherent sidelobe averaging for nonrepeating waveforms [5].

It was recently shown [7] that MiCRFt can be extended to contend with cross-correlation sidelobes that arise in a multiple-input multiple-output (MIMO) context for operation involving shared time/frequency support. For waveforms having a "thumbtack" ambiguity function [8], an appreciable Doppler shift essentially amounts to another distinct waveform; meaning that the MIMO extension of MiCRFt suggests utility for Doppler expansion as well. The design of Doppler-robust MMFs (on a per-pulse basis) was explored in [17]. Further, [18] examined compensation for straddling and intrapulse Doppler. With similar motivation, a Doppler-resilient extension to MiCRFt for complementary operation is proposed here.

In keeping with the nomenclature for DG-Comp-FM waveform design, we hereby develop the Doppler-Generalized MiCRFt (DG-MiCRFt) framework to enable complementary sidelobe cancellation (CSC) across a prescribed Doppler span, noting that slow-time presumming inherently collapses unambiguous Doppler to $\pm\pi/Z$ radians/pulse. Furthermore, it is shown that this broadening of the CSC-span is equivalent to applying a covariance matrix taper (CMT) to the original zero-Doppler MiCRFt formulation. Consequently, direct parallels can be drawn from robust beamforming approaches in which CMTs likewise produce a wider cancellation span to compensate for spatial straddling/uncertainty of interference [9].

II. LS-MMF AND MICRFT FOR FM WAVEFORMS

Consider baseband FM waveform $s(t)$ that is "oversampled" by factor K relative to bandwidth B (i.e., $F_s = KB$) to realize the length-N vector $\mathbf{s} = [s_0 \quad s_1 \quad \cdots \quad s_{N-1}]^T$. Then, the length-$L$ least-squares mismatched filter (LS-MMF) $\mathbf{h}$ can be obtained by minimizing the difference between the filter output and some desired response $\mathbf{d}$ [10], via

This work was supported by the Office of Naval Research under Contract #N00014-23-C-1053. DISTRIBUTION STATEMENT A. Approved for Public Release.

$$\min_{\mathbf{h}} \|\mathbf{A}\mathbf{h} - \mathbf{d}\|_2^2 + \delta\|\mathbf{h}\|_2^2 . \quad (1)$$

The parameter δ (≥ 0) is a regularization term that provides some control of mismatch loss, and $\mathbf{A}$ is a $(L+N-1)\times L$ convolution matrix of the form

$$\mathbf{A} = \begin{bmatrix} s_0 & 0 & \cdots & 0 \\ \vdots & s_0 & & \vdots \\ s_{N-1} & \vdots & \ddots & 0 \\ 0 & s_{N-1} & & s_0 \\ \vdots & & \ddots & \vdots \\ 0 & \cdots & 0 & s_{N-1} \end{bmatrix} \quad (2)$$

in which $L = MN$ represents an "overlengthening" (by M) factor relative to the waveform dimensionality. While any deviation from standard matched filtering poses some degree of mismatch loss, both the inclusion of δ and the specific choice of $\mathbf{d}$ can largely ameliorate such effects. Efficient computational methods to achieve precise desired MML are examined in [11]. Here, $\mathbf{d}$ is defined as the nominal matched-filter mainlobe, which facilitates the necessary beam spoiling to prevent a super-resolution condition that otherwise induces severe MML [12].

The closed-form least-squares (LS) solution to (1) is

$$\mathbf{h} = (\mathbf{A}^H\mathbf{A} + \delta\mathbf{I})^{-1}\mathbf{A}^H\mathbf{d}, \quad (3)$$

where $\mathbf{I}$ is an $L\times L$ identity matrix, $(\cdot)^H$ is the Hermitian operation, and δ now serves as a diagonal-loading factor.

While the per-pulse LS solution above suppresses range sidelobes to the degree possible with L design degrees-of-freedom (DoF), expanding to include the presumming of Z *unique* responses increases design dimensionality to LZ, such that complementary-on-receive operation is realized. These MiCRFt filters [6] are formulated as the solution to

$$\min_{\overline{\mathbf{h}}} \left\|\overline{\mathbf{A}}\overline{\mathbf{h}} - Z\mathbf{d}\right\|_2^2 + \delta\left\|\overline{\mathbf{h}}\right\|_2^2, \quad (4)$$

with $\overline{\mathbf{A}}$ the $(L+N-1)\times LZ$ block-convolution matrix $\overline{\mathbf{A}} = [\mathbf{A}_0 \quad \mathbf{A}_1 \quad \cdots \quad \mathbf{A}_{Z-1}]$, for $\mathbf{A}_z$ the convolution matrix for the z^{th} unique FM waveform per (2). Similarly, the term $\overline{\mathbf{h}}$ is the $LZ\times 1$ concatenation of Z length-L filters. Like (3), the solution to (4) is solved in closed form to be

$$\overline{\mathbf{h}} = Z\left(\overline{\mathbf{A}}^H\overline{\mathbf{A}} + \delta\overline{\mathbf{I}}\right)^{-1}\overline{\mathbf{A}}^H\mathbf{d}, \quad (5)$$

where $\overline{\mathbf{I}}$ is a $LZ \times LZ$ identity matrix and the $(k,i)^{\text{th}}$ block of the block-matrix inner-product is $[\overline{\mathbf{A}}^H\overline{\mathbf{A}}]_{k,i} = \mathbf{A}_k^H\mathbf{A}_i$ (i.e., the cross-correlation matrix between the k^{th} and i^{th} waveforms $\mathbf{s}_k$ and $\mathbf{s}_i$). This method relies on the Z waveforms being unique; otherwise (5) simplifies to (3). The degree of uniqueness is important, as insufficient distinction could likewise lead to deterioration back to (3).

III. Doppler-Generalized MiCRFt

The original MiCRFt formulation addresses the zero-Doppler condition, with range-sidelobe cancellation achieved for stationary scattering and degrading relatively quickly with deviation from that model. To suppress range-sidelobes across a band of U non-zero Doppler shifts, consider the modified LS formulation

$$\min_{\overline{\mathbf{h}}} \left\|\widetilde{\mathbf{A}}\overline{\mathbf{h}} - Z\tilde{\mathbf{d}}\right\|_2^2 + \delta\left\|\overline{\mathbf{h}}\right\|_2^2, \quad (6)$$

where $\bar{\mathbf{h}}$ is the same concatenated filter structure as in (5), and the $(L+N-1)U \times LZ$ matrix

$$\widetilde{\mathbf{A}} = \frac{1}{\sqrt{U}}\begin{bmatrix} \mathbf{A}_0 & \mathbf{A}_1 e^{j\omega_0} & \cdots & \mathbf{A}_{Z-1}e^{j(Z-1)\omega_0} \\ \mathbf{A}_0 & \mathbf{A}_1 e^{j\omega_1} & \cdots & \mathbf{A}_{Z-1}e^{j(Z-1)\omega_1} \\ \vdots & \vdots & \ddots & \vdots \\ \mathbf{A}_0 & \mathbf{A}_1 e^{j\omega_{U-1}} & \cdots & \mathbf{A}_{Z-1}e^{j(Z-1)\omega_{U-1}} \end{bmatrix} \quad (7)$$

collects convolution matrices for U Doppler responses across the Z-pulse subset. The term

$$\tilde{\mathbf{d}} = \left[\frac{\mathbf{1}_Z^T\mathbf{v}(\omega_0)}{Z}\mathbf{d}^T \quad \ldots \quad \frac{\mathbf{1}_Z^T\mathbf{v}(\omega_{U-1})}{Z}\mathbf{d}^T\right]^T \quad (8)$$

is a length $(L+N-1)U$ concatenated desired response vector and the Doppler manifold across the waveform subset is described by

$$\mathbf{v}(\omega) = [e^{j\omega(0)} \quad e^{j\omega(1)} \quad \ldots \quad e^{j\omega(Z-1)}]^T. \quad (9)$$

The $\mathbf{1}_Z$ term is a Z-length vector of ones (corresponding to the zero-Doppler manifold) such that the scaling $\mathbf{1}_Z^T\mathbf{v}(\omega_u)/Z$ on each term in (8) corresponds to the Doppler mainlobe roll-off caused by presumming mismatch between zero and non-zero Doppler shifts.

The least-squares solution to (6) is thus

$$\overline{\mathbf{h}} = Z\left(\widetilde{\mathbf{A}}^H\widetilde{\mathbf{A}} + \delta\overline{\mathbf{I}}\right)^{-1}\widetilde{\mathbf{A}}^H\tilde{\mathbf{d}}, \quad (10)$$

which upon filtering and presumming, achieves complementary range-sidelobe suppression across the slow-time Doppler band established by (7) and (8).

While the matrix inversion is still of identical size $LZ\times LZ$, the number of Doppler points U determines the number of block-rows in $\widetilde{\mathbf{A}}$, with higher U significantly adding to the computational load in the determination of $\overline{\mathbf{h}}$. However, as $U\to\infty$, the $(k,i)^{\text{th}}$ block-component matrix $\widetilde{\mathbf{A}}^H\widetilde{\mathbf{A}}$ simplifies significantly to

$$\begin{aligned} \lim_{U\to\infty}\left[\widetilde{\mathbf{A}}^H\widetilde{\mathbf{A}}\right]_{k,i} &= \lim_{U\to\infty}\left(\frac{1}{U}\sum_{u} e^{j(i-k)\omega_u}\right)\mathbf{A}_k^H\mathbf{A}_i \\ &= \frac{1}{2W}\int_{-W}^{W} e^{j(i-k)\omega}d\omega\,\mathbf{A}_k^H\mathbf{A}_i \\ &= \operatorname{sinc}\big(W(i-k)\big)\,\mathbf{A}_k^H\mathbf{A}_i\,, \end{aligned} \quad (11)$$

where W is the desired width of the complementary Doppler span. Hence, this DG-MiCRFt filter is equivalent to a tapered solution to the original MiCRFt formulation and can therefore be implemented with the same order of complexity (aside from the sinc multiplication in (11)). Likewise, the k^{th} block-vector portion of $\widetilde{\mathbf{A}}^H\overline{\mathbf{d}}$ simplifies to

$$\begin{aligned} &\lim_{U\to\infty}\left[\widetilde{\mathbf{A}}^H\tilde{\mathbf{d}}\right]_k \\ &= \lim_{U\to\infty}\frac{1}{Z}\sum_{u=0}^{U-1}\mathbf{A}_k^H\mathrm{e}^{-jk\omega_u}\big(\mathbf{1}^T\mathbf{v}(\omega_u)\big)\mathbf{d} \\ &= \mathbf{A}_k^H\mathbf{d}\frac{1}{Z}\sum_{z=0}^{Z-1}\frac{1}{2W}\int_{-W}^{W} e^{j(z-k)\omega}d\omega \\ &= \mathbf{A}_k^H\mathbf{d}\left(\frac{1}{Z}\sum_{z=0}^{Z-1}\operatorname{sinc}[W(z-k)]\right). \end{aligned} \quad (12)$$

With these simplifications, the DG-MiCRFt filters can be equivalently written as a modification of the zero-Doppler form in (5) as

$$\overline{\mathbf{h}} = Z\left(\left[\overline{\mathbf{T}}\odot\overline{\mathbf{A}}^H\overline{\mathbf{A}}\right] + \delta\overline{\mathbf{I}}\right)^{-1}\left[\bar{\mathbf{t}}\odot\overline{\mathbf{A}}^H\mathbf{d}\right] \quad (13)$$

where the matrix

$$\overline{\mathbf{T}} = \mathbf{T} \otimes \mathbf{1}_{L\times L} \tag{14}$$

is a Toeplitz-block sinc matrix taper as $[\mathbf{T}]_{i,k} = \mathrm{sinc}\big(W(i-k)\big)$, and

$$\bar{\mathbf{t}} = \mathbf{t} \otimes \mathbf{1}_{L\times 1} \tag{15}$$

is a block-taper with $\mathbf{t} = \frac{1}{Z}\mathbf{T}\mathbf{1}_{Z\times 1}$ the average of columns in $\mathbf{T}$. This result is similar to that of covariance matrix tapering (CMT) in beamforming, where interference mismatch is addressed via broadened nulls at the beamformer output [13][14]. Indeed, the motivation behind the DG-MiCRFt methodology is to achieve a Doppler-broadened "cancellation condition" that follows the same notion. The general trend indicates that increasing Z has the benefit of lowering range sidelobes within the span of W at the cost of shrinking unambiguous Doppler space. Due to presumming, in which the unambiguous Doppler space is reduced by a factor of Z, the desired complementary span should not exceed $W_{\max} = 1/Z$, which would cause complementary cancellation for the entire reduced Doppler space of $\omega_{\mathrm{d}} \in \left(-\frac{\pi}{Z}, \frac{\pi}{Z}\right)$.

While the original MiCRFt approach achieves complementary cancellation with $\mathcal{O}((LZ)^3)$ complexity due to the matrix inversion (which can be determined off-line), the DG-MiCRFt approach could be realized by incorporating an additional $U-1$ Doppler-shifted versions into the formulation. However, due to DG-MiCRFt being equivalent to a tapered solution to the original problem, there is no significant additional computational cost in the determination of these filters.

IV. Mismatch Loss

The LS formulae described above enable complementary range-sidelobe cancellation as a trade-off for some mismatch loss relative to matched filtering that maximizes signal-to-noise-ratio (SNR). As such, consideration of the total degree of loss is necessary. First, to enable consistent comparison between filters, begin by normalizing each MMF and matched filter (MF) to produce unity noise gain at the filter output, which is achieved through the rescaling operation [6]

$$\overline{\mathbf{h}} \leftarrow \frac{\overline{\mathbf{h}}}{\frac{1}{Z}\sqrt{(\overline{\mathbf{h}}^H\overline{\mathbf{h}})(\bar{\mathbf{s}}^H\bar{\mathbf{s}})}}. \tag{16}$$

Here, $\bar{\mathbf{s}} = [\mathbf{s}_0^T \quad \mathbf{s}_2^T \quad \dots \quad \mathbf{s}_{Z-1}^T]^T$ is the $LZ\times 1$ concatenation of Z discretized waveforms, where each signal $\mathbf{s}_z$ is zero-padded equally on either side from length N to length L. In a similar fashion, $\overline{\mathbf{h}}_{\mathrm{MF}}$ is the $LZ\times 1$ concatenation of zero-padded matched filters. The normalization in (16) is similar to that of the LS-MMF normalization of (3), the main differences being the sum of multiple filters and corresponding waveforms, as well as the scalar $1/Z$ resulting from presumming. The mismatch-loss for a given filter subset is thus

$$\mathrm{MML}\big(\overline{\mathbf{h}}\big) = \frac{\left|\overline{\mathbf{h}}^H\bar{\mathbf{s}}\right|^2}{\left(\overline{\mathbf{h}}^H\overline{\mathbf{h}}\right)(\bar{\mathbf{s}}^H\bar{\mathbf{s}})}. \tag{17}$$

Since DG-MiCRFt seeks to achieve complementary range-sidelobe cancellation for scattering within some non-zero Doppler span, it is also instructive to consider losses due to Doppler mismatch. The above-mentioned MML is filter-dependent, quantifying losses at zero-Doppler only. The total mismatch loss $L_{\mathrm{SNR}}\big(\overline{\mathbf{h}},\omega\big)$ is quantified in terms of both filter loss and complementary model mismatch between the assumed zero-Doppler manifold $\mathbf{v}(\omega=0) = \mathbf{1}_Z$ and the expanded Doppler manifold $\mathbf{v}(\omega)$ from (8). The total mismatch loss is therefore

$$L_{\mathrm{SNR}}\big(\overline{\mathbf{h}},\omega\big) = \frac{\left|\overline{\mathbf{h}}^H([\mathbf{v}(\omega)\otimes\mathbf{1}_L]\odot\bar{\mathbf{s}})\right|^2}{\left(\overline{\mathbf{h}}^H\overline{\mathbf{h}}\right)(\bar{\mathbf{s}}^H\bar{\mathbf{s}})}. \tag{18}$$

Note that even for the matched filter, complementary processing is indicative of some loss due to the implied sinc mask imposed across Doppler, thus reducing the observable Doppler space by $\pm\pi/Z$ radians/pulse.

V. Simulation Analysis

To assess the performance of DG-MiCRFt, $Q = 50$ subsets of $Z = 4$ random FM waveforms (totaling $P = 200$) are evaluated. Each signal is unique, such that complementary cancellation is enabled at the subset-level and additional incoherent sidelobe cancellation (ISC) is obtained at the CPI-level [6] (regular slow-time processing). The waveforms employed are produced via the pseudo-random optimized FM (PRO-FM) framework, spectrally shaped to a super-Gaussian of order 4 to obtain a near-rectangular passband, each with $TB = 64$, and oversampled by $K = 4$ relative to the 6-dB bandwidth [15]. Both the MiCRFt and DG-MiCRFt filters are designed with an $M = 4$ filter extension factor and diagonal loading δ dynamically set to be 30 dB below the average waveform energy of each subset.

Per-subset evaluation across Doppler is achieved by examining the Z-pulse cross point-spread function (CPSF)

$$\Psi(\tau,\omega_{\mathrm{d}}) = \frac{1}{Z}\sum_{z=0}^{Z-1}(\mathbf{s}_z \star \mathbf{h}_z)e^{-j\omega_{\mathrm{d}}zT_{\mathrm{PRI}}}, \tag{19}$$

where T_{PRI} is the uniform pulse-repetition interval and $\star$ is a correlation operation performed between signal/filter pairs, followed by standard Doppler processing [16]. Evaluation of (19) is therefore indicative of "per-subset" range sidelobe performance as a function of Doppler, while $\Psi(\tau,0)$ quantifies the zero-Doppler pre-summed response.

Fig. 1 shows the root mean-squared (RMS) CPSF across all $Q = 50$ subsets, formed via the zero-Doppler version of MiCRFt from (5), i.e., $W = 0$. Here, the evaluation of

$$\text{RMS response} = \sqrt{\frac{1}{Q}\sum_{q=0}^{Q-1}\left|\Psi_q(\tau,\omega_{\mathrm{d}})\right|^2} \tag{20}$$

shows the average per-subset performance due to MiCRFt filtering. The magenta traces denote the resulting unambiguous Doppler interval due to presumming, while the zero lag cut demonstrates the anticipated SNR loss from (18) across Doppler. Similarly, Fig. 2 evaluates

$$\text{Coherent mean} = \left|\frac{1}{Q}\sum_{q=0}^{Q-1}\Psi_q(\tau,\omega_{\mathrm{d}})\right|^2, \tag{21}$$

which is indicative of "per-CPI" performance, where additional incoherent sidelobe averaging is observed due to unique waveform subsets. Apparent in either plot, the complementary "span" of $W = 0$ MiCRFt filtering is quite narrow, as indicated by the null at zero Doppler. Thus, non-stationary scattering

would not benefit from the same degree of sidelobe cancellation as experienced at zero Doppler.

Next, employing DG-MiCRFt filters ($W = 0.25$), the RMS and coherent mean responses of the CPSF across all $Q = 50$ subsets are shown in Figs. 3 and 4, respectively. Clearly, DG-MiCRFt significantly broadens the Doppler span over which a complementary benefit is achieved. However, the null depth is shallower as a consequence.

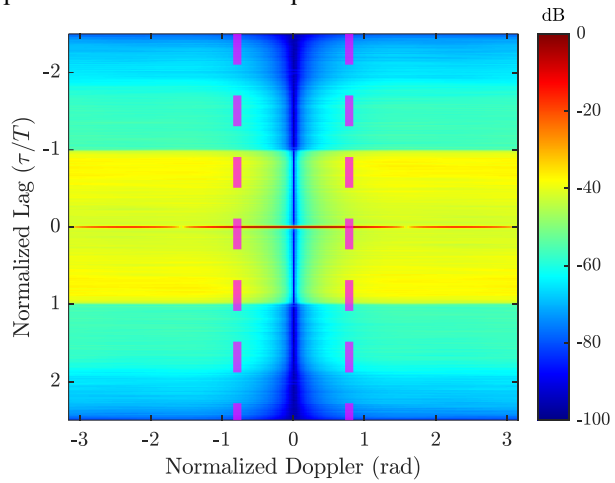

Fig. 1. Per-subset $Q = 50$, $W = 0$ (MiCRFt) RMS range sidelobe profile across Doppler

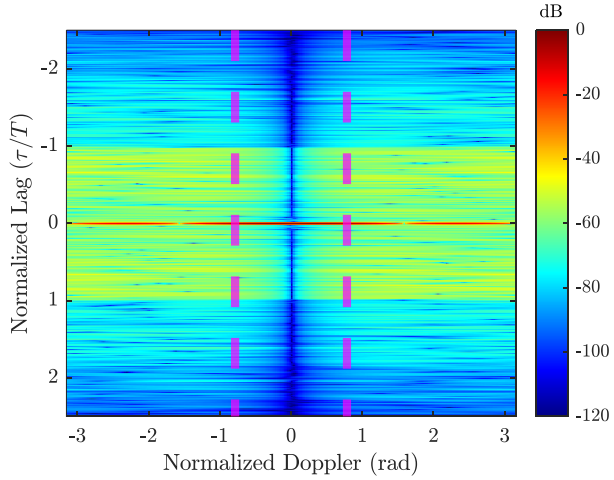

Fig. 2. Per-CPI $Q = 50$, $W = 0$ (MiCRFt) mean range sidelobe profile across Doppler

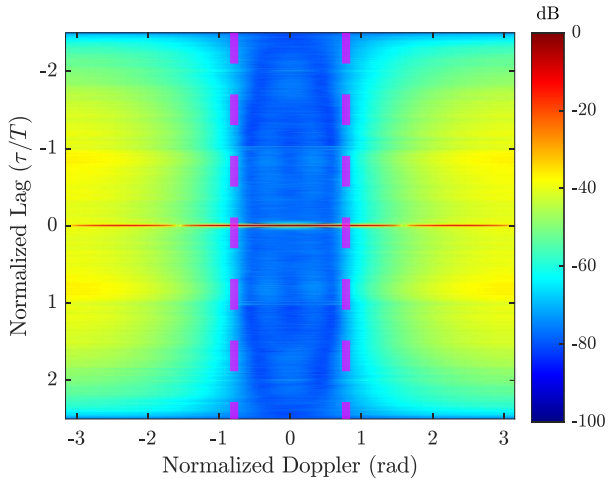

Fig. 3. Per-subset $Q = 50$, $W = 0.25$ (DG-MiCRFt) RMS range sidelobe profile across Doppler

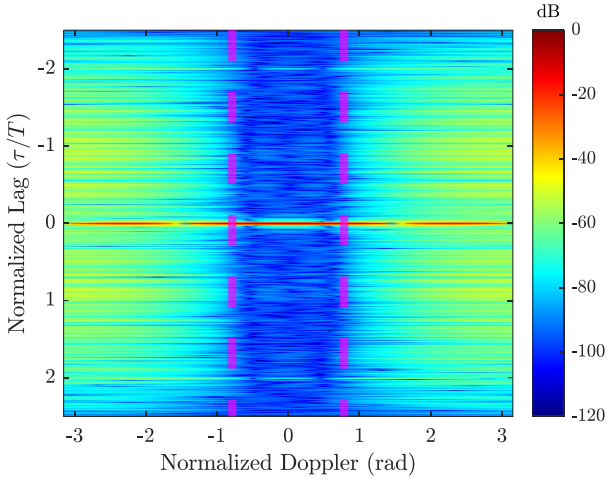

Fig. 4. Per-CPI $Q = 50$, $W = 0.25$ (DG-MiCRFt) mean range sidelobe profile across Doppler

The zero-Doppler cuts from Figs. 1 and 3 are shown in Fig. 5, illustrating the RMS performance of both filters at zero-Doppler. For comparison, the standard MF and LS-MMF performance from (3) are also shown (applied on a per-pulse basis and presummed by the same factor of Z). Note that the peaks of each method exhibit the anticipated SNR loss from (17) due to evaluation at zero-Doppler specifically. Here, the average MML exhibited by MiCRFt is 2.4 dB, while that of DG-MiCRFt is 3.0 dB and LS-MMF is 3.1 dB when evaluated at zero-Doppler.

Compared to the MF and LS-MMF, which produce an integrated sidelobe level (ISL) of -13.2 dB and -30.5 dB (on average) respectively, MiCRFt and the Doppler-Generalized extension thereof further reduce sidelobes to ISL values of -62.39 dB and -48.68 dB, respectively, when evaluated at zero-Doppler. Therefore, the improvement of MiCRFt and DG-MiCRFt is roughly 49 dB and 36 dB when compared to standard matched filtering, while relative to LS-MMF the improvement is 32 dB and 18 dB. The tradeoff between MiCRFt and DG-MiCRFt is that the latter bears higher sidelobes and increased mismatch loss in exchange for sidelobe cancellation over a wider Doppler span.

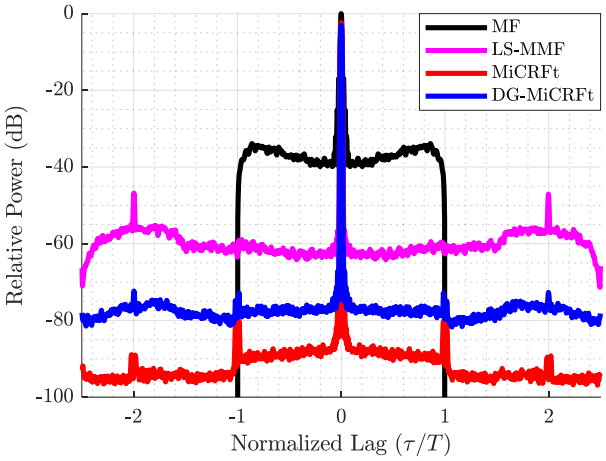

Fig. 5. RMS filter outputs for $Q = 50$ subsets formed with the matched, least squares, MiCRFt, and DG-MiCRFt filters

The average MML of the DG-MiCRFt filter subsets when optimized for different W (using the same $Q = 50$ subsets) is shown in Fig. 6. Any non-zero W leads to higher MML, demonstrating that DG-MiCRFt incurs more loss than its predecessor. Of course, increasing diagonal loading δ leads to decreased MML across all of W at the expense of increasing ISL.

Fig. 7 displays the ISL versus Doppler when the DG-MiCRFt filters are optimized with various unique Doppler null widths W (applied to the same waveforms with the same parameters), demonstrating an additional tradeoff between achievable ISL and complementary-span. Immediately after the Doppler deviates to $\omega_d = 0.05$, the ISL of the MiCRFt filter ($W = 0$) becomes significantly higher than that of the other DG-MiCRFt cases. With increasing Doppler null width W, the Doppler bandwidth over which the ISL remains fixed is predictably expanded, allowing for some degree of customization if the designer is anticipating a maximum Doppler bandwidth for the given system and operating environment (i.e. airborne radar).

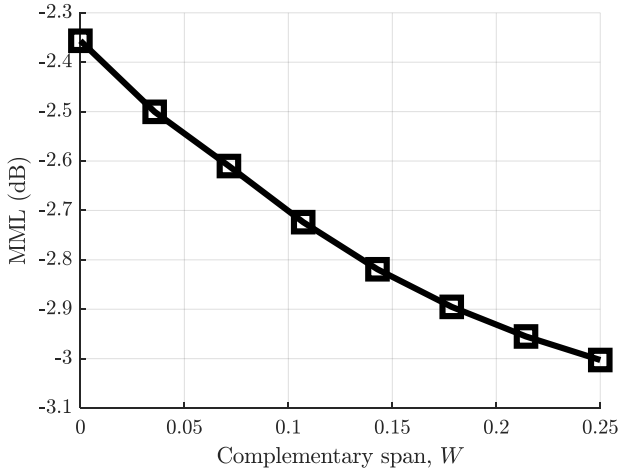

Fig. 6. Mean mismatch loss as a function of Doppler null width W for a fixed diagonal loading factor set 30 dB below the average waveform energy of each subset

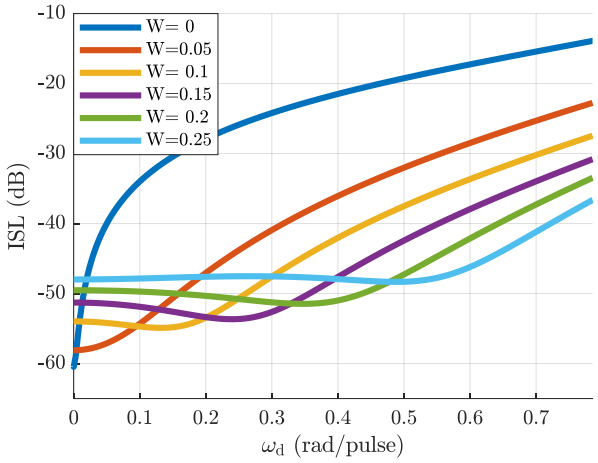

Fig. 7. Integrated sidelobe level (ISL) versus inter-pulse Doppler ω_d for DG-MiCRFt filters of varying complementary spans

VI. Experimental Results

Using hardware in a loopback configuration, the same $P = 200$ waveforms from Section V are captured. The waveforms are generated using a Tektronix AWG 70002A at 3.4 GHz, passed through a VBFZ-3590+ filter to mitigate Nyquist images, and amplified via TVA-82-213. The "transmitted" signal is attenuated, filtered again via VBFZ-3590+, and amplified with a ZX60-3800LN+ low noise amplifier prior to capture with a spectrum analyzer. Fig. 8 displays the pulse-compressed responses when presumming using the same filters as in Fig. 5. Here, it is observed that MiCRFt exhibits 2.4 dB of MML, while DG-MiCRFt and LS-MMF exhibit 3.0 dB and 3.1 dB of MML for a zero-Doppler shifted signal, respectively. Indeed, a small loss of 0.006 dB is noted for the MF as well due to the modest transmitter distortion of this arrangement.

In Fig. 9, the loopback waveforms are artificially subjected to a normalized Doppler shift of $\omega_d = 0.2\pi$ after capture to demonstrate the expanded robustness of DG-MiCRFt compared to MiCRFt. Due to the non-negligible Doppler shift, the complementary assumption of MiCRFt is violated, causing significant sidelobe degradation (approaching the MF), while DG-MiCRFt exhibits nearly the same sidelobe levels as in Fig. 8 due to compensation during design. The *total* mismatch loss (i.e., MML + loss due to presumming like in (18)) is now increased due to the Doppler shift, which is likewise observable in the MF result (note that the MF peak is now -2.3 dB). Indeed, the remaining MMF, MiCRFt, and DG-MiCRFt filters experience similar losses due to Doppler mismatch, in addition to MML due to deviation from the matched filter.

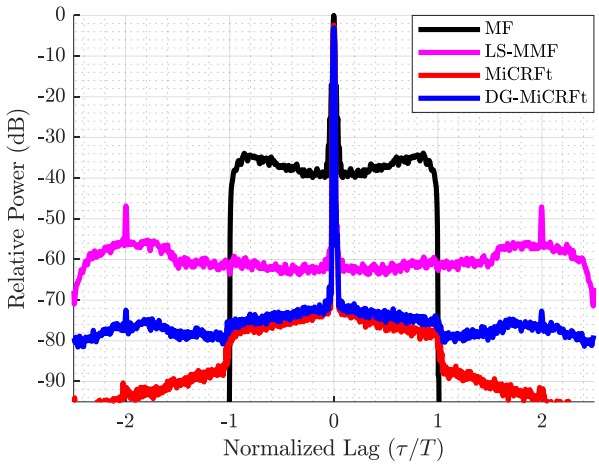

Fig. 8. RMS filter outputs for $Q = 50$ subsets formed with the matched, least squares, MiCRFt, and DG-MiCRFt filters. Waveforms are captured in loopback.

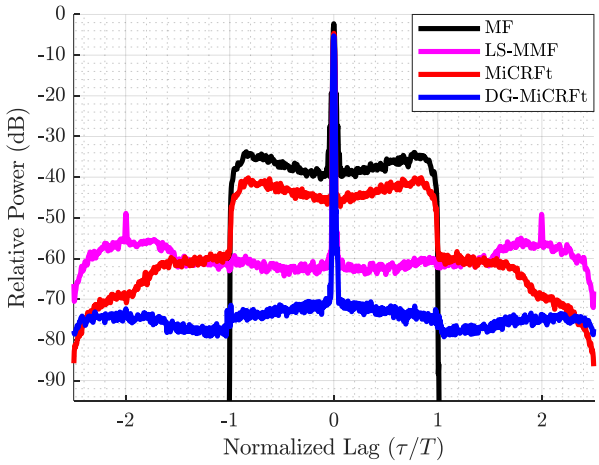

Fig. 9. RMS filter outputs for $Q = 50$ subsets formed with the matched, least squares, MiCRFt, and DG-MiCRFt filters. Waveforms are captured in loopback and artificially Doppler-shifted by $\omega_d = 0.2\pi$.

VII. Conclusions

The DG-MiCRFt method has been experimentally demonstrated via loopback measurements to provide complementary benefits for scatterer responses over a predefined Doppler span. In comparison to MiCRFt, which is capable of achieving very low sidelobe suppression for zero-Doppler, DG-MiCRFt some cancellation enhancement for an expanded Doppler span. Both methods reduce integrated sidelobe levels at the cost of slightly increased mismatch loss.

References

[1] M. Golay, "Complementary series," *IEEE Trans. Info. Theory*, vol. 7, no. 2, pp. 82–87, Apr. 1961.

[2] N. Levanon, I. Cohen, P. Itkin, "Complementary pair radar waveforms–evaluating and mitigating some drawbacks," *IEEE Aerospace & Electronic Systems Mag.*, vol. 32, no. 3, pp. 40-50, Mar. 2017.

[3] A. Pezeshki, A. Calderbank, W. Moran, S. Howard, "Doppler resilient Golay complementary waveforms," *IEEE Trans. Info. Theory*, vol. 54, no. 9, pp. 4254-4266, Sept. 2008.

[4] Z. Wu, C. X. Wang, P. Jiang, Z. Zhou, "Range-doppler sidelobe suppression for pulsed radar based on Golay complementary codes," *IEEE Signal Processing Letters*, vol. 27, pp. 1205-1209, July 2020.

[5] D. Felton, J. Owen, M. Heintzelman, D. Herr, S. Blunt, "Improving doppler robustness for optimized complementary FM waveform subsets," *Intl. Radar Conf.*, Rennes, France, Oct. 2024.

[6] C. Jones, C. Mohr, P. McCormick, S. Blunt, "Complementary frequency modulated radar waveforms and optimised receive processing". *IET Radar, Sonar, Navigation*, vol. 15, no. 7, pp. 708-723, Apr. 2021.

[7] M. Heintzelman, C. Jones, P. McCormick, S. Blunt, "Mismatched complementary-on-receive filtering (MiCRFt) for MIMO radar," *IEEE Radar Conf.*, Denver, CO, May 2024.

[8] N. Levanon, Eli Mozeson, "Radar Signals", IEEE, 2004.

[9] T. Cuprak and K. Wage, "Efficient Doppler-Compensated Reiterative Minimum Mean-Squared-Error Processing," in *IEEE Trans. on Aerospace and Electronic Systems*, vol. 53, no. 2, pp. 562-574, April 2017.

[10] M. Ackroyd, F. Ghani, "Optimum mismatched filters for sidelobe suppression," *IEEE Trans. Aerospace & Electronic Systems*, vol. AES-9, no. 2, pp. 214-218, Mar. 1973.

[11] C. Jones, P. McCormick, M. Heintzelman, "Computationally efficient constraint-optimized radar mismatched filtering for waveform-agile systems," *IEEE Trans. Aerospace & Electronic Systems*, vol. 61, no. 3, pp. 6711-6732, June 2025.

[12] M. Heintzelman, J. Owen, S. Blunt, B. Maio, E. Steinbach, "Practical considerations for optimal mismatched filtering of nonrepeating waveforms," *IEEE Radar Conf.*, San Antonio, TX, May 2023.

[13] H. Van Trees, *Optimum Array Processing*, John Wiley & Sons, 2002.

[14] J. Guerci, "Theory and application of covariance matrix tapers for robust adaptive beamforming," *IEEE Trans. Signal Processing*, vol. 47, no. 4, pp. 977-985, Apr. 1999.

[15] M. Heintzelman, T. Kramer, S. Blunt, "Experimental evaluation of super-Gaussian-shaped random FM waveforms," *IEEE Radar Conf.*, New York City, NY, Mar. 2022.

[16] M. Richards, J. Scheer, W. Holm, eds., *Principles of Modern Radar: Basic Principles*, 1st ed., SciTech Publishing, 2010.

[17] M.-E. Chatzitheodoridi, A. Taylor, O. Rabaste, "A mismatched filter for integrated sidelobe level minimization over a continuous Doppler shift interval," *IEEE Radar Conf.*, Florence, Italy, Sep. 2020.

[18] O. Rabaste, J. Bosse, "Robust mismatched filter for off-grid target," *IEEE Signal Processing Letters*, vol. 26, no. 8, pp. 1147-1151, Aug. 2019.